Rapid Communications

Dispersive magnetic and electronic excitations in iridate perovskites probed by oxygen *K*-edge resonant inelastic x-ray scattering

Xingye Lu,[1,*] Paul Olalde-Velasco,[1,†] Yaobo Huang,[1] Valentina Bisogni,[1,‡] Jonathan Pelliciari,[1,§] Sara Fatale,[2] Marcus Dantz,[1] James G. Vale,[3] E. C. Hunter,[4] Johan Chang,[5,‖] Vladimir N. Strocov,[1] R. S. Perry,[6,7] Marco Grioni,[2] D. F. McMorrow,[3] Henrik M. Rønnow,[5] and Thorsten Schmitt[1,¶]

[1]*Research Department Synchrotron Radiation and Nanotechnology, Paul Scherrer Institut, CH-5232 Villigen PSI, Switzerland*
[2]*Institute of Physics, École Polytechnique Fédérale de Lausanne (EPFL), CH-1015 Lausanne, Switzerland*
[3]*London Centre for Nanotechnology and Department of Physics and Astronomy, University College London, Gower Street, London WC1E 6BT, United Kingdom*
[4]*School of Physics and Astronomy, The University of Edinburgh, James Clerk Maxwell Building, Mayfield Road, Edinburgh EH9 2TT, United Kingdom*
[5]*Laboratory for Quantum Magnetism, Institute of Physics, École Polytechnique Fédérale de Lausanne (EPFL), CH-1015 Lausanne, Switzerland*
[6]*ISIS Neutron Spallation Source, Rutherford Appleton Laboratory (RAL), Harwell Campus, Didcot OX11 0QX, United Kingdom*
[7]*London Centre for Nanotechnology and UCL Centre for Materials Discovery, University College London, 17-19 Gordon Street, London WC1H 0AH, United Kingdom*

(Received 4 August 2017; published 3 January 2018; corrected 2 February 2018)

Resonant inelastic x-ray scattering (RIXS) experiments performed at the oxygen K edge on the iridate perovskites Sr_2IrO_4 and $Sr_3Ir_2O_7$ reveal a sequence of well-defined dispersive modes over the energy range up to ∼0.8 eV. The momentum dependence of these modes and their variation with the experimental geometry allows us to assign each of them to specific collective magnetic and/or electronic excitation processes, including single and bimagnons, and spin-orbit and electron-hole excitons. We thus demonstrate that dispersive magnetic and electronic excitations are observable at the O K edge in the presence of the strong spin-orbit coupling in the 5d shell of iridium and strong hybridization between Ir 5d and O 2p orbitals, which confirm and expand theoretical expectations. More generally, our results establish the utility of O K-edge RIXS for studying the collective excitations in a range of 5d materials that are attracting increasing attention due to their novel magnetic and electronic properties. Especially, the strong RIXS response at O K edge opens up the opportunity for investigating collective excitations in thin films and heterostructures fabricated from these materials.

DOI: 10.1103/PhysRevB.97.041102

Characterizing the elementary excitations in correlated electron systems is an essential prerequisite for obtaining a complete understanding of the underlying electronic interactions and therefore crucial for revealing the origin of emergent phases [1,2]. Resonant inelastic x-ray scattering (RIXS) has become established in the past decade as a powerful tool for studying the momentum dependence of electronic and magnetic excitations [2]. Of particular interest is RIXS at the transition-metal (TM) $L_{2,3}$ edges. Because of the strong spin-orbit coupling (SOC) in the $2p_{\frac{3}{2},\frac{1}{2}}$ level of the intermediate state, single spin-flip excitations are directly allowed at TM $L_{2,3}$ edges [3–5], making TM $L_{2,3}$ RIXS especially suited for investigating the magnetic dynamics in 3d (cuprates and iron pnictides) [3–14] and 5d (iridates and osmates) systems [15–19].

While the Mott state in cuprates is dominated by a strong on-site electron correlation (U), the $J_{\text{eff}} = \frac{1}{2}$ Mott state in $5d^5$ iridates is driven by collaborative strong SOC (∼0.5 eV) and intermediate U (∼2 eV) under a strong octahedral crystal electric field [20]. Because of their novel Mott physics and certain parallelism with cuprates, layered iridates (Sr_2IrO_4 and $Sr_3Ir_2O_7$) have attracted substantial research interest [15–18,20–22] [Figs. 1(a)–1(c)]. More recently, thin films and heterostructures of perovskite iridates have been suggested to host nontrivial topological states [23–25] and triggered a new wave of studies on artificial structures [26–28]. However, measuring elementary excitations using Ir L RIXS on artificial low-dimensional samples requires a longer counting time than that on bulk crystal because 11.2 keV of the x ray has ∼10 μm [29] of attenuation length while artificial thin

*Present address: Department of Physics, Beijing Normal University, Beijing 100875, China; xingye.lu@psi.ch
†Present address: Instituto de Física, Benemérita Universidad Autónoma de Puebla, Apdo. Postal J-48, Puebla, Puebla 72570, México.
‡Present address: National Synchrotron Light Source II, Brookhaven National Laboratory, Upton, New York 11973, USA.
§Present address: Department of Physics, Massachusetts Institute of Technology, Cambridge, Massachusetts 02139, USA.
‖Present address: Physik-Institut, Universität Zürich, Winterthurerstrasse 190, CH-8057, Zürich, Switzerland.
¶thorsten.schmitt@psi.ch

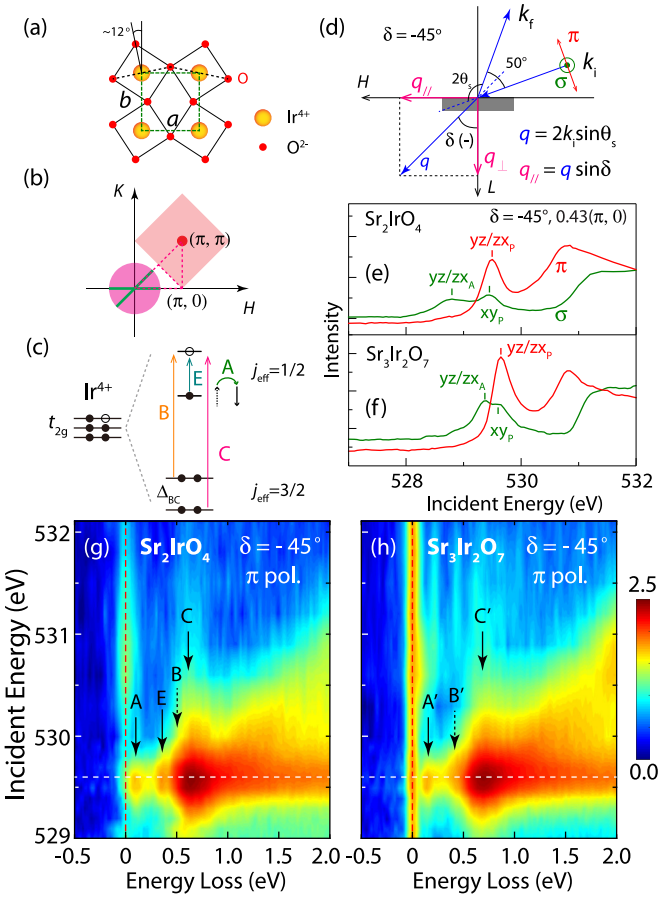

FIG. 1. (a) Schematic of the distorted IrO plane of Sr_2IrO_4 and $Sr_3Ir_2O_7$. (b) The corresponding reciprocal space in tetragonal notation. The solid pink circle around the Γ point is the momentum coverage of O K RIXS with $2\theta_s = 130°$. The solid green lines mark the two directions $[H,0]$ and $[H,H]$ we measured. (c) Schematic of elementary excitations of iridates in a single-ion picture. A denotes the single magnon, B and C spin-orbit excitons, and E the electron-hole exciton. Δ_{BC} marks the energy difference between B and C. (d) Schematics of the backscattering RIXS experimental setup. The blue arrows k_i and k_f denote the incident and scattered photons, where the polarizations are shown as a red arrow (π) and a green dotted circle (σ). The scattering angle is $2\theta_s = 130°$. The projections of q onto two reciprocal axes ($q_\parallel$ and $q_\perp$) can be tuned continuously by changing δ. (e) and (f) X-ray absorption spectra at a grazing-incidence angle ($\delta = -45°$) along $[H,0]$. The probed Ir t_{2g} orbitals (xy, yz, and zx) are marked, where the subscripts A and P indicate that orbitals are probed via their hybridization with apical or plane oxygens. (g) and (h) Incident-energy dependence of the elementary excitations of Sr_2IrO_4 and $Sr_3Ir_2O_7$, measured near the O K edge with π polarization and $\delta = -45°$ along $[H,0]$.

films and superlattices are usually much thinner (~10-100 nm) [7,8,27,28].

RIXS at the O K edge (O 1s to O 2p, ~530 eV) offers unique opportunities in probing the elementary excitations in 4d and 5d TM oxides [30,31] with high-energy resolution (~45 meV) [32,33]. Although O K RIXS has a much smaller attenuation length ($\lesssim$100 nm) than Ir L RIXS, a comparison between O K and Ir L_3 spectra measured on Sr_2IrO_4 suggests that they have a comparable counting efficiency (see Fig. S6 in the Supplemental Material [34]). Therefore, soft x-ray RIXS is a promising method for studying artificial two-dimensional samples [7,8]. However, given that SOC is absent in the O 1s level, O K RIXS is expected to be insensitive to single spin-flip excitations [31,35,36]. This would severely limit the applicability of O K RIXS on iridates and related 5d TM oxides, especially thin films and heterostructures fabricated by these materials, where magnetic excitations need to be studied for probing the low-energy Hamiltonian [15–18].

Although SOC is absent in the O 1s orbital, it exists in the Ir 5d shell which strongly hybridizes with O 2p orbitals. This could allow single spin-flip processes at the O K edge. Indeed, Kim *et al.* [37] proposed that single spin-flip excitations will be intense at the Γ point for O K RIXS if strong SOC is present in TM d orbitals and space inversion symmetry at the oxygen sites is broken. However, the symmetry analysis in Ref. [37] is only viable for $q = 0$ and π of a one-dimensional distorted Ir_1-O_1-Ir_2-O_2 periodic arrangement [black dashed line in Fig. 1(a)], which is far from the situations for real iridate materials, such as the perovskite layered iridates (Sr_2IrO_4 and $Sr_3Ir_2O_7$) bearing special interests. Later, O K RIXS measurements on a Sr_2IrO_4 thin film reported the possible observation of single magnons at low q, but failed to observe the corresponding dispersion that can conclusively determine the single-magnon nature of the observed signal [38]. Therefore, the capability of O K RIXS in probing the magnetic excitations of iridates remains to be explored experimentally. In addition, the origin of some collective modes being important for understanding the charge dynamics is still under debate [16,39] and requires further experimental studies.

In this Rapid Communication, we use O K RIXS to study the layered perovskite iridates Sr_2IrO_4 and $Sr_3Ir_2O_7$ (the $n = 1$ and 2 of the Ruddlesden-Popper series $Sr_{n+1}Ir_nO_{3n+1}$), which exhibit novel $J_{\text{eff}} = \frac{1}{2}$ Mott physics [16,20,40,41]. We unambiguously observe the single-magnon dispersion of both samples, thus providing conclusive evidence for the capability of O K RIXS in probing single magnons in 5d TM oxides with large SOC. The collective excitonic quasiparticles dispersing between 0.4 and 0.6 eV at the Ir L_3 edge of Sr_2IrO_4 [16] "dressed" by magnons [37] have also been observed at the O K edge of Sr_2IrO_4 and $Sr_3Ir_2O_7$. Our results thereby establish the capabilities of O K RIXS in studying dispersive magnetic and electronic excitations in iridates and manifest the strong Ir 5d-O 2p hybridization in these materials. In addition, the dimensionality and temperature dependence of the excitations in Sr_2IrO_4 and $Sr_3Ir_2O_7$ indicate an electron-hole exciton nature of the sharp dispersive mode [E in Fig. 1(g)].

The Sr_2IrO_4 and $Sr_3Ir_2O_7$ single crystals used in this study were grown by the flux method [42,43]. The x-ray absorption (XAS) and RIXS measurements were carried out at the ADRESS beamline of the Swiss Light Source at the Paul Scherrer Institut [44], with both π and σ polarizations [Fig. 1(d)]. The scattering angle was set to $2\theta_s = 130°$, by which a substantial area of the first Brillouin zone is accessible [pink circle in Fig. 1(b)]. The measurements were performed along two high-symmetry directions $[H,0]$ and $[H,H]$ in tetragonal notation with $a = b \approx 3.9$ Å. The energy resolution for the RIXS measurements was set to 65 meV. The in-plane momentum $q_\parallel$ can be tuned continuously by rotating the sample and thereby changing the angle (δ) [Fig. 1(d)].

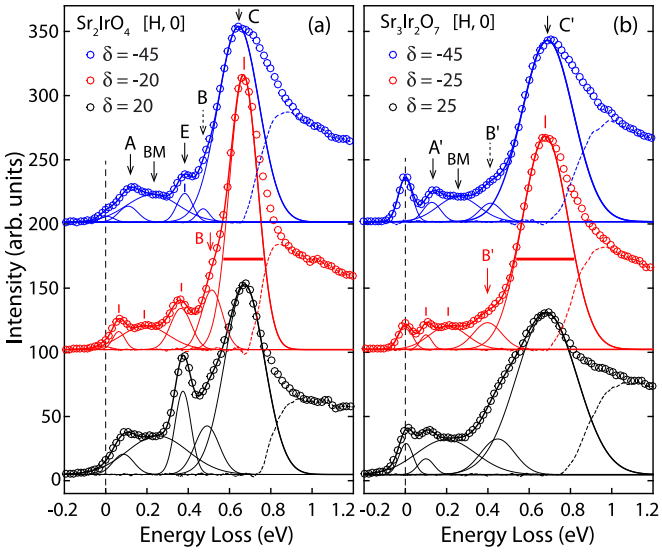

FIG. 2. Multi-Gaussian fitting of the RIXS spectra for (a) Sr_2IrO_4 and (b) $Sr_3Ir_2O_7$. The spectra at three different δ's are shown as open colored circles. From low- to high-energy loss, the Gaussian peaks (solid curves) denote the elastic peak (centered at zero energy loss), single magnon (A/A′), bimagnon (BM), electron-hole exciton (E), excitonic quasiparticle (B/B′), and spin-orbit exciton (C/C′). The dashed curves are the residual weight of the fitting.

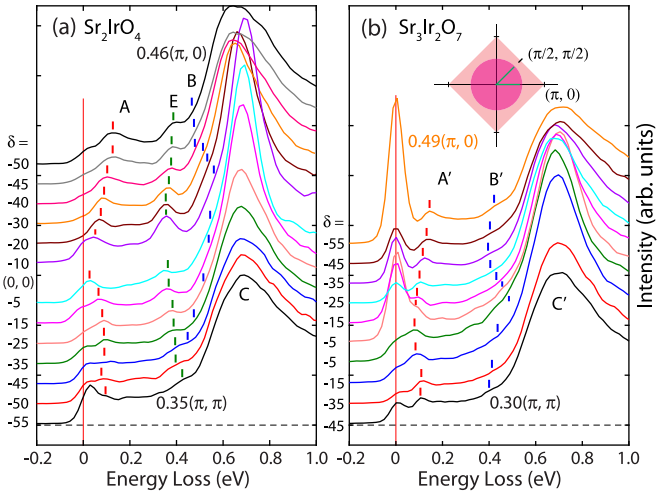

FIG. 3. Momentum-dependent RIXS spectra along $[H,0]$ and $[H,H]$ directions for (a) Sr_2IrO_4 and (b) $Sr_3Ir_2O_7$. The inset in (b) illustrates the reciprocal space, where the pink diamond is the magnetic Brillouin zone and the solid pink circle the momentum coverage by O K RIXS. The green lines are the $[H,0]$ and $[H,H]$ high-symmetry directions for RIXS measurements. The red vertical lines mark the zero energy loss positions. The red, green, and blue markers indicate the fitted peak energies of the single magnons (A/A′), the electron-hole excitons (E), and the excitonic quasiparticles (B/B′), respectively.

Figures 1(e) and 1(f) show the XAS spectra for Sr_2IrO_4 and $Sr_3Ir_2O_7$ measured at a grazing-incidence angle ($\delta = -45°$) [$\mathbf{Q} = 0.43(\pi,0)$] using π and σ polarizations. The polarization dependence is determined by the hybridization between Ir $5d$ t_{2g} and O $2p$ orbitals and the matrix elements of the O $1s$-$2p$ dipole transitions. The σ polarization probes Ir $5d$ yz/zx (xy) orbitals hybridized with $2p_x/2p_y$ orbitals of apical (plane) oxygens. The π polarization predominantly favors the Ir $5d$ yz/zx orbitals via plane-oxygen $2p_z$ orbitals [20,30,31]. After having determined the K-edge resonant energies for plane and apical oxygens [yz/zx_A, xy_P, and yz/zx_P in Figs. 1(e) and 1(f)], we have performed incident-energy-dependent RIXS measurements covering these resonant energies. The results measured with π polarization are shown in Figs. 1(g) and 1(h). Clear Raman peaks A/A′, E, and C/C′ observed below 1 eV are identified as single magnons, electron-hole excitons across the charge gap, and spin-orbit excitons, respectively [Fig. 1(c)]. B/B′ and BM resolved via multi-Gaussian fitting are spin-orbit excitons "dressed" by magnons and bimagnons, respectively [Fig. 1(c)].

Figure 2 shows the fitting of selected spectra from grazing incidence [$\delta = -45°$, $0.43(\pi,0)$] to normal incidence [$\delta = 25°$, $0.25(\pi,0)$] for Sr_2IrO_4 and $Sr_3Ir_2O_7$ using multiple Gaussians. The systematic fitting resolves all the collective modes below 1 eV and shows their incident-angle-dependent cross sections. To identify the nature of these collective modes, we have measured the momentum dependence of the RIXS spectra along $[H,0]$ and $[H,H]$ for both Sr_2IrO_4 and $Sr_3Ir_2O_7$ (Fig. 3), with the incident photon energy tuned to the resonant energy yz/zx_P that enhances all the Raman modes. The spectra shown in Figs. 2 and 3 are normalized to the charge transfer excitations between 5 and 11 eV [34]. It is remarkable that A and A′ show clear dispersions with energy gaps around $\mathbf{Q} = (0,0)$. The extracted dispersions from the fitting coincide with the magnon dispersions measured by Ir L_3 RIXS for both Sr_2IrO_4 and $Sr_3Ir_2O_7$ (Fig. 4) [15–18]. Without any doubt, A and A′ can be attributed to single magnons, proving that O K RIXS is sensitive to single magnons in the iridates with strong SOC in the $5d$ shell and broken inversion symmetry at the oxygen sites [37]. The large magnon gap (~90 meV) in $Sr_3Ir_2O_7$ was explained to be driven by the strong magnetic anisotropy associated with SOC [17,18]. The smaller magnon gap in Sr_2IrO_4 (~40 meV) is consistent with an Ir L_3 RIXS report [16] and was described by including an XY anisotropic term [45,46] into the Heisenberg model described in Ref. [15]. Besides the dispersions, we find that the single magnons persist in the whole momentum space measured with undiminished spectral weight (Figs. 2 and 3), therefore sorting out the momentum dependence of the magnon intensity, which was not settled in previous studies [37,38].

The fitting in Fig. 2 reveals a broad spectral structure at ~200 meV for both Sr_2IrO_4 and $Sr_3Ir_2O_7$ (blue squares in Fig. 4), which show similar dispersions to the corresponding single magnons. This feature can be attributed to bimagnons, because (1) their energy scales are consistent with the bimagnons (160 meV for Sr_2IrO_4 and 185 meV for $Sr_3Ir_2O_7$) measured by Raman scattering [47] and (2) their dispersions are in agreement with those measured by Ir L_3 RIXS [16–18]. Note that the bimagnons of cuprates measured by O K RIXS are nondispersive [35,36]. The presence of both single magnons and bimagnons indicates that O K RIXS is a powerful spectroscopic method for studying the magnetic dynamics of iridates.

In addition to the magnetic excitations, O K RIXS also reveals the dispersive spin-orbit excitons (B and C) in Sr_2IrO_4

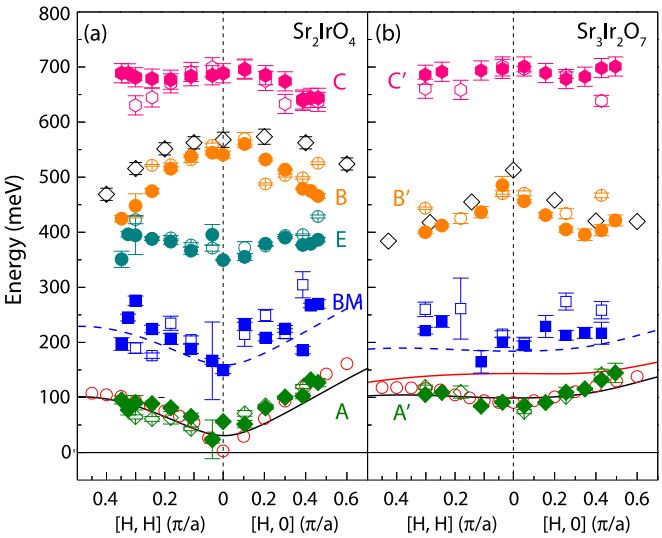

FIG. 4. Dispersions of the collective modes in (a) Sr_2IrO_4 and (b) $Sr_3Ir_2O_7$ probed by O K RIXS. From low- to high-energy loss, the green diamonds, blue squares, cyan circles, orange circles, and pink hexagons denote the single magnons (A/A′), bimagnons (BM), electron-hole excitons (E), spin-orbit excitons creating magnons (B/B′), and spin-orbit excitons (C/C′), respectively. The solid and open symbols are extracted from the spectra with $\delta < 0$ and $\delta > 0$, respectively (Figs. 1 and 2). The open red circles are the single-magnon energies extracted from previous Ir L_3 RIXS measurements [15,18]. The open black diamonds denote the dispersions of the excitonic quasiparticles extracted from Refs. [16,50]. The black curve in (a) is a theoretical fit of the magnon dispersion using a Heisenberg model reported in Refs. [45,46]. The black and red curves in (b) are transverse and longitudinal magnon dispersions for $Sr_3Ir_2O_7$ using the quantum-dimer model reported in Ref. [18]. The blue dashed curves are the expected lower bound of the bimagnon continuum.

[Fig. 1(c)] as observed in previous Ir L_3 RIXS experiments [16,48]. C can be easily attributed to a spin-orbit exciton mode (at ∼0.7 eV) [17,18,49] that exhibits a minor dispersion and strong intensity [16,48]. The mode B finds direct correspondence with the excitonic quasiparticle (spin-orbit exciton "dressed" by magnons) reported in Ref. [16], because of their coincidence in dispersion [Fig. 4(a)] and similarities in bandwidth [Figs. 2(a) and 4(a)]. Furthermore, the intensity of B increases while approaching normal incidence from grazing incidence [Fig. 2(a)]. This incident-geometry dependence of intensity is also consistent with that for the excitonic quasiparticles [16] and therefore corroborates this identification. The spin-orbit exciton modes B and C arise from the electronic transitions from the $j = \frac{3}{2}$ quartet to $j = \frac{1}{2}$ doublet, with B arising mainly from the $|j = 3/2, j_z = \pm 3/2\rangle$ doublet, while C bears mostly $|j = 3/2, j_z = \pm 1/2\rangle$ character. The energy difference between B and C ($\Delta_{BC} \approx 150$ meV) reflects the splitting of the $j = \frac{3}{2}$ band, which is caused by the tetragonal distortion of the IrO_6 octahedra [16].

A similar analysis can be applied to the collective modes B′ and C′ in $Sr_3Ir_2O_7$. The mode B′ is the excitonic quasiparticle in $Sr_3Ir_2O_7$ and C′ the spin-orbit exciton mode at higher energy (∼0.7 eV). B′ and C′ show similar dispersions to B and C, indicating similar origins and behaviors. However, the energy widths of B′ and C′ are larger than that for B and C, as evidenced from our fitting analysis in Fig. 2. This larger bandwidth is caused by the increase in dimensionality (more adjacent IrO_6 octahedra) in $Sr_3Ir_2O_7$ [51]. The energy of B′ is obviously lower than B, meaning that the splitting of the $j = \frac{3}{2}$ states in $Sr_3Ir_2O_7$ is larger ($\Delta_{B'C'} \approx 200$ meV), indicating a larger tetragonal distortion field in $Sr_3Ir_2O_7$ [16,52].

The sharp collective mode E below 0.4 eV is an intriguing feature whose origin is still under debate [16,39]. It was first suggested to be an electron-hole exciton at the edge of the electron-hole continuum, which has a threshold at about 0.41 eV [16,52,53] [Fig. 1(c)]. Alternatively, it was explained as driven by a Jahn-Teller effect with strong SOC [39]. In our measurements, E decreases in intensity with increasing temperature and disappears at 300 K (Fig. S7 of the Supplemental Material [34]). This is consistent with the decrease and broadening of the electron-hole continuum threshold at high temperatures, as indicated by optical conductivity measurements [53]. The absence of E in $Sr_3Ir_2O_7$ (Figs. 2 and 3) can also be unified in this exciton picture, as the much smaller charge insulating gap (∼130 meV) and the broader bandwidth of $Sr_3Ir_2O_7$ could smear this exciton and push it to a lower energy (∼100 meV) [51,54].

The excitonic quasiparticles B and B′ ($|j = 3/2, j_z = \pm 3/2\rangle$ to $|j = 1/2, j_z = \pm 1/2\rangle$) deserve special attention. The propagation of the excitonic quasiparticles in the antiferromagnetic context creates flipped spins along their hopping path [16]. Moreover, B and B′ are magnetic dd excitations in nature. From the selection rules for dipolar transitions, $\Delta j_z = 0, \pm 1$, it follows that B/B′ contains only spin-1 magnetic components, which usually rotate the photon polarization by $\pi/2$, the same as the single spin-flip excitations. This is consistent with previous theoretical calculations [37], which also generate magnetic dd excitations within the 5d t_{2g} orbitals of Sr_2IrO_4. Therefore, we conclude that the excitonic quasiparticles observed by O K RIXS are magnetic orbital excitations "dressed" by magnons. The spin-orbit exciton mode C/C′ consists of both nonmagnetic and magnetic components.

The capability of O K RIXS in probing magnetic excitations in iridates is driven by the strong SOC in the Ir 5d shell and hybridization between the Ir 5d t_{2g} and O 2p orbitals because spin is not a good quantum number in Ir 5d t_{2g} states, and indirect electronic transitions between Ir 5d t_{2g} orbitals and O 1s states via strong O 2p-Ir 5d hybridization allow flipping of the $j = \frac{1}{2}$ pseudospin and changing of the $j = \frac{3}{2}$ states, in which the former induce single magnons and the latter magnetic (and nonmagnetic) dd excitations. The role of the space inversion symmetry breaking at oxygen sites needs further O K RIXS studies on iridate systems with different Ir-O-Ir bond angles.

In conclusion, our results on Sr_2IrO_4 and $Sr_3Ir_2O_7$ and their comparison with previous Ir L_3 RIXS results have established the capability of O K RIXS in probing single magnons and excitonic quasiparticles over a substantial part of the first Brillouin zone of layered iridates, which host strong SOC-entangled states in 5d orbitals. O K RIXS has a high-energy resolution for studying most 5d TM oxides [33]. Since O K RIXS usually generates a strong RIXS response within a small attenuation length, its unique capabilities in probing elementary excitations provide a different method for investigating 5d TM oxides, especially for artificial thin films, heterostructures, and superlattices.

The work at PSI and EPFL is supported by the Swiss National Science Foundation through its Sinergia network Mott Physics Beyond the Heisenberg Model (MPBH). The work in London is supported by the U.K. Engineering and Physical Sciences Research Council (Grants No. EP/N027671/1 and No. EP/N034694/1). X.L., V.B., and P.O.-V. acknowledge financial support from the European Community's Seventh Framework Program (FP7/2007-2013) under Grant Agreement No. 290605 (COFUND: PSI-FELLOW). J.P. and T.S. acknowledge financial support through the Dysenos AG by Kabelwerke Brugg AG Holding, Fachhochschule Nordwestschweiz, and the Paul Scherrer Institut. J.P. acknowledge financial support by the Swiss National Science Foundation Early Postdoc, Mobility fellowship Project No. P2FRP2_171824. The work at PSI is partially funded by the Swiss National Science Foundation through the D-A-CH program (SNSF Research Grant No. 200021L 141325). H.M.R. acknowledges financial support from SNSF Grant No. 200020-166298. P.O.-V. acknowledges financial support for the work at Puebla Mexico from SEP (511-6/17-8017) PTC-553 and VIEP-BUAP (OLVP-exc17).

[1] P. W. Anderson, *Basic Notions of Condensed Matter Physics* (Benjamin Cummings, London, 1984).

[2] L. J. P. Ament, M. van Veenendaal, T. P. Devereaux, J. P. Hill, and J. van den Brink, Rev. Mod. Phys. **83**, 705 (2011).

[3] L. J. P. Ament, G. Ghiringhelli, M. Moretti Sala, L. Braicovich, and J. van den Brink, Phys. Rev. Lett. **103**, 117003 (2009).

[4] L. Braicovich, L. J. P. Ament, V. Bisogni, F. Forte, C. Aruta, G. Balestrino, N. B. Brookes, G. M. De Luca, P. G. Medaglia, F. Miletto Granozio, M. Radovic, M. Salluzzo, J. van den Brink, and G. Ghiringhelli, Phys. Rev. Lett. **102**, 167401 (2009).

[5] L. Braicovich, J. van den Brink, V. Bisogni, M. Moretti Sala, L. J. P. Ament, N. B. Brookes, G. M. De Luca, M. Salluzzo, T. Schmitt, V. N. Strocov, and G. Ghiringhelli, Phys. Rev. Lett. **104**, 077002 (2010).

[6] M. Le Tacon, G. Ghiringhelli, J. Chaloupka, M. Moretti Sala, V. Hinkov, M. W. Haverkort, M. Minola, M. Bakr, K. J. Zhou, S. Blanco-Canosa, C. Monney, Y. T. Song, G. L. Sun, C. T. Lin, G. M. De Luca, M. Salluzzo, G. Khaliullin, T. Schmitt, L. Braicovich, and B. Keimer, Nat. Phys. **7**, 725 (2011).

[7] M. P. M. Dean R. S. Springell, C. Monney, K. J. Zhou, J. Pereiro, I. Božović, B. Dalla Piazza, H. M. Rønnow, E. Morenzoni, J. van den Brink, T. Schmitt, and J. P. Hill, Nat. Mater. **11**, 850 (2012).

[8] M. P. M. Dean, G. Dellea, R. S. Springell, F. Yakhou-Harris, K. Kummer, N. B. Brookes, X. Liu, Y-J. Sun, J. Strle, T. Schmitt, L. Braicovich, G. Ghiringhelli, I. Božović, and J. P. Hill, Nat. Mater. **12**, 1019 (2013).

[9] W. S. Lee, J. J. Lee, E. A. Nowadnick, S. Gerber, W. Tabis, S. W. Huang, V. N. Strocov, E. M. Motoyama, G. Yu, B. Moritz, H. Y. Huang, R. P. Wang, Y. B. Huang, W. B. Wu, C. T. Chen, D. J. Huang, M. Greven, T. Schmitt, Z. X. Shen, and T. P. Devereaux, Nat. Phys. **10**, 883 (2014).

[10] J. Schlappa, K. Wohlfeld, K. J. Zhou, M. Mourigal, M. W. Haverkort, V. N. Strocov, L. Hozoi, C. Monney, S. Nishimoto, S. Singh, A. Revcolevschi, J.-S. Caux, L. Patthey, H. M. Rønnow, J. van den Brink, and T. Schmitt, Nature (London) **485**, 82 (2012).

[11] K.-J. Zhou, Y.-B. Huang, C. Monney, X. Dai, V. N. Strocov, N.-L. Wang, Z.-G. Chen, C. Zhang, P. Dai, L. Patthey, J. van den Brink, H. Ding, and T. Schmitt, Nat. Commun. **4**, 1470 (2013).

[12] C. J. Jia, E. A. Nowadnick, K. Wohlfeld, Y. F. Kung, C.-C. Chen, S. Johnston, T. Tohyama, B. Moritz, and T. P. Devereaux, Nat. Commun. **5**, 3314 (2014).

[13] M. Guarise, B. Dalla Piazza, H. Berger, E. Giannini, T. Schmitt, H. M. Rønnow, G. A. Sawatzky, J. van den Brink, D. Altenfeld, I. Eremin, and M. Grioni, Nat. Commun. **5**, 5760 (2014).

[14] C. Monney, T. Schmitt, C. E. Matt, J. Mesot, V. N. Strocov, O. J. Lipscombe, S. M. Hayden, and J. Chang, Phys. Rev. B **93**, 075103 (2016).

[15] J. Kim, D. Casa, M. H. Upton, T. Gog, Y.-J. Kim, J. F. Mitchell, M. van Veenendaal, M. Daghofer, J. van den Brink, G. Khaliullin, and B. J. Kim, Phys. Rev. Lett. **108**, 177003 (2012).

[16] J. Kim, M. Daghofer, A. H. Said, T. Gog, J. van den Brink, G. Khaliullin, and B. J. Kim, Nat. Commun. **5**, 4453 (2014).

[17] J. Kim, A. H. Said, D. Casa, M. H. Upton, T. Gog, M. Daghofer, G. Jackeli, J. van den Brink, G. Khaliullin, and B. J. Kim, Phys. Rev. Lett. **109**, 157402 (2012).

[18] M. Moretti Sala, V. Schnells, S. Boseggia, L. Simonelli, A. Al-Zein, J. G. Vale, L. Paolasini, E. C. Hunter, R. S. Perry, D. Prabhakaran, A. T. Boothroyd, M. Krisch, G. Monaco, H. M. Ronnow, D. F. McMorrow, and F. Mila, Phys. Rev. B **92**, 024405 (2015).

[19] S. Calder, J. G. Vale, N. A. Bogdanov, X. Liu, C. Donnerer, M. H. Upton, D. Casa, A. H. Said, M. D. Lumsden, Z. Zhao, J.-Q. Yan, D. Mandrus, S. Nishimoto, J. van den Brink, J. P. Hill, D. F. McMorrow, and A. D. Christianson, Nat. Commun. **7**, 11651 (2016).

[20] B. J. Kim, H. Jin, S. J. Moon, J.-Y. Kim, B.-G. Park, C. S. Leem, J. Yu, T. W. Noh, C. Kim, S.-J. Oh, J.-H. Park, V. Durairaj, G. Cao, and E. Rotenberg, Phys. Rev. Lett. **101**, 076402 (2008).

[21] B. J. Kim, H. Ohsumi, T. Komesu, S. Sakai, T. Morita, H. Takagi, and T. Arima, Science **323**, 1329 (2009).

[22] J. W. Kim, Y. Choi, J. Kim, J. F. Mitchell, G. Jackeli, M. Daghofer, J. van den Brink, G. Khaliullin, and B. J. Kim, Phys. Rev. Lett. **109**, 037204 (2012).

[23] D. Xiao, W. Zhu, Y. Ran, N. Nagaosa, and S. Okamoto, Nat. Commun. **2**, 596 (2011).

[24] Y. Chen, Y.-M. Lu, and H.-Y. Kee, Nat. Commun. **6**, 6593 (2015).

[25] C. Fang, L. Lu, J. Liu, and L. Fu, Nat. Phys. **12**, 936 (2016).

[26] J. Matsuno, K. Ihara, S. Yamamura, H. Wadati, K. Ishii, V. V. Shankar, H.-Y. Kee, and H. Takagi, Phys. Rev. Lett. **114**, 247209 (2015).

[27] A. Lupascu, J. P. Clancy, H. Gretarsson, Zixin Nie, J. Nichols, J. Terzic, G. Cao, S. S. A. Seo, Z. Islam, M. H. Upton, J. Kim, D. Casa, T. Gog, A. H. Said, V. M. Katukuri, H. Stoll, L. Hozoi, J. van den Brink, and Y.-J. Kim, Phys. Rev. Lett. **112**, 147201 (2014).

[28] J. H. Gruenewald, J. Kim, H. S. Kim, J. M. Johnson, J. Hwang, M. Souri, J. Terzic, S. H. Chang, A. Said, J. W. Brill, G. Cao, H.-Y. Kee, and S. S. A. Seo, Adv. Mater. **29**, 1603798 (2017).

[29] B. L. Henke, E. M. Gullikson, and J. C. Davis, At. Data Nucl. Data Tables **54**, 181 (1993).

[30] M. Moretti Sala, M. Rossi, S. Boseggia, J. Akimitsu, N. B. Brookes, M. Isobe, M. Minola, H. Okabe, H. M. Ronnow, L. Simonelli, D. F. McMorrow, and G. Monaco, Phys. Rev. B **89**, 121101(R) (2014).

[31] C. G. Fatuzzo, M. Dantz, S. Fatale, P. Olalde-Velasco, N. E. Shaik, B. Dalla Piazza, S. Toth, J. Pelliciari, R. Fittipaldi, A. Vecchione, N. Kikugawa, J. S. Brooks, H. M. Rønnow, M. Grioni, Ch. Rüegg, T. Schmitt, and J. Chang, Phys. Rev. B **91**, 155104 (2015).

[32] W. S. Lee, S. Johnston, B. Moritz, J. Lee, M. Yi, K. J. Zhou, T. Schmitt, L. Patthey, V. Strocov, K. Kudo, Y. Koike, J. van den Brink, T. P. Devereaux, and Z. X. Shen, Phys. Rev. Lett. **110**, 265502 (2013).

[33] The energy resolution of the O K-edge RIXS of SAXES spectrometer at ADRESS beamline is ∼45 meV with a reasonable counting rate. For even higher-energy resolving power, see the descriptions of ID32 at ESRF, SIX at NSLS II, and I21 at Diamond.

[34] See Supplemental Material at http://link.aps.org/supplemental/10.1103/PhysRevB.97.041102 for details.

[35] V. Bisogni, L. Simonelli, L. J. P. Ament, F. Forte, M. Moretti Sala, M. Minola, S. Huotari, J. van den Brink, G. Ghiringhelli, N. B. Brookes, and L. Braicovich, Phys. Rev. B **85**, 214527 (2012).

[36] V. Bisogni, M. Moretti Sala, A. Bendounan, N. B. Brookes, G. Ghiringhelli, and L. Braicovich, Phys. Rev. B **85**, 214528 (2012).

[37] B. H. Kim and J. van den Brink, Phys. Rev. B **92**, 081105(R) (2015).

[38] X. Liu, M. P. M. Dean, J. Liu, S. G. Chiuzbăian, N. Jaouen, A. Nicolaou, W. G. Yin, C. Rayan Serrao, R. Ramesh, H. Ding, and J. P. Hill, J. Phys.: Condens. Matter **27**, 202202 (2015).

[39] E. M. Plotnikova, M. Daghofer, J. van den Brink, and K. Wohlfeld, Phys. Rev. Lett. **116**, 106401 (2016).

[40] G. Jackeli and G. Khaliullin, Phys. Rev. Lett. **102**, 017205 (2009).

[41] J. G. Rau, E. K.-H. Lee, and H.-Y. Kee, Annu. Rev. Condens. Matter Phys. **7**, 195 (2016).

[42] G. Cao, J. Bolivar, S. McCall, J. E. Crow, and R. P. Guertin, Phys. Rev. B **57**, R11039 (1998).

[43] G. Cao, Y. Xin, C. S. Alexander, J. E. Crow, P. Schlottmann, M. K. Crawford, R. L. Harlow, and W. Marshall, Phys. Rev. B **66**, 214412 (2002).

[44] G. Ghiringhelli, A. Piazzalunga, C. Dallera, G. Trezzi, L. Braicovich, T. Schmitt, V. N. Strocov, R. Betemps, L. Patthey, X. Wang, and M. Grioni, Rev. Sci. Instrum. **77**, 113108 (2006).

[45] J. G. Vale, S. Boseggia, H. C. Walker, R. Springell, Z. Feng, E. C. Hunter, R. S. Perry, D. Prabhakaran, A. T. Boothroyd, S. P. Collins, H. M. Rønnow, and D. F. McMorrow, Phys. Rev. B **92**, 020406(R) (2015).

[46] D. Pincini, J. G. Vale, C. Donnerer, A. de la Torre, E. C. Hunter, R. Perry, M. Moretti Sala, F. Baumberger, and D. F. McMorrow, Phys. Rev. B **96**, 075162 (2017).

[47] H. Gretarsson, N. H. Sung, M. Höppner, B. J. Kim, B. Keimer, and M. Le Tacon, Phys. Rev. Lett. **116**, 136401 (2016).

[48] H. Gretarsson, N. H. Sung, J. Porras, J. Bertinshaw, C. Dietl, J. A. N. Bruin, A. F. Bangura, Y. K. Kim, R. Dinnebier, J. Kim, A. Al-Zein, M. Moretti Sala, M. Krisch, M. Le Tacon, B. Keimer, and B. J. Kim, Phys. Rev. Lett. **117**, 107001 (2016).

[49] X. Lu, D. E. McNally, M. Moretti Sala, J. Terzic, M. H. Upton, D. Casa, G. Ingold, G. Cao, and T. Schmitt, Phys. Rev. Lett. **118**, 027202 (2017).

[50] S. Bossegia, Ph.D. thesis, University College London, 2014, pp. 184 and 193.

[51] S. J. Moon, H. Jin, K. W. Kim, W. S. Choi, Y. S. Lee, J. Yu, G. Cao, A. Sumi, H. Funakubo, C. Bernhard, and T. W. Noh, Phys. Rev. Lett. **101**, 226402 (2008).

[52] H. Gretarsson, J. P. Clancy, X. Liu, J. P. Hill, E. Bozin, Y. Singh, S. Manni, P. Gegenwart, J. Kim, A. H. Said, D. Casa, T. Gog, M. H. Upton, H.-S. Kim, J. Yu, V. M. Katukuri, L. Hozoi, J. van den Brink, and Y.-J. Kim, Phys. Rev. Lett. **110**, 076402 (2013).

[53] S. J. Moon, H. Jin, W. S. Choi, J. S. Lee, S. S. A. Seo, J. Yu, G. Cao, T. W. Noh, and Y. S. Lee, Phys. Rev. B **80**, 195110 (2009).

[54] Y. Okada, D. Walkup, H. Lin, C. Dhital, T.-R. Chang, S. Khadka, W. Zhou, H.-T. Jeng, M. Paranjape, A. Bansil, Z. Wang, S. D. Wilson, and V. Madhavan, Nat. Mater. **12**, 707 (2013).

Correction: A present address footnote was inserted for the tenth author.